

## Fast Inhomogeneous Plane Wave Algorithm for Homogeneous Dielectric Body of Revolution

Xi Rui<sup>1,2</sup>, Jun Hu<sup>1</sup> and Qing Huo Liu<sup>2,\*</sup>

<sup>1</sup> School of Electronic Engineering, University of Electronic Science and Technology of China, Chengdu, Sichuan 610054, China.

<sup>2</sup> Department of Electrical and Computer Engineering, Duke University, Durham, NC 27708, USA.

Received 22 September 2009; Accepted (in revised version) 14 December 2009

Available online 17 May 2010

---

**Abstract.** To solve the electromagnetic scattering problem for homogeneous dielectric bodies of revolution (BOR), a fast inhomogeneous plane wave algorithm is developed. By using the Weyl identity and designing a proper integration path, the aggregation and disaggregation factors can be derived analytically. Compared with the traditional method of moments (MoM), both the memory and CPU time requirements are reduced for large-scale homogeneous dielectric BOR problems. Numerical results are given to demonstrate the validity and the efficiency of the proposed method.

**AMS subject classifications:** 35Q61, 74F15, 74J20, 83C50

**Key words:** Bodies of revolution, fast inhomogeneous plane wave algorithm, electromagnetic scattering.

---

## 1 Introduction

The electromagnetic radiation and scattering from a body of revolution (BOR) of an arbitrary shape have been widely discussed during last several decades. BOR objects of various types, including perfect electric conductors, homogeneous dielectric bodies, coated conducting bodies and combined dielectric and conducting bodies have been studied [1–11]. Because of the axial symmetry of the geometry, only the generatrix that forms the surface of the model is needed for solving the BOR problem in a surface integral equation formulation. Both the memory requirement and the CPU time are reduced compared with the full three-dimensional method [12]. In the BOR integral equation solver, the incident plane wave is expanded in cylindrical modes. The induced current

---

\*Corresponding author. *Email address:* qhliu@ee.duke.edu (Q. H. Liu)

of each mode is solved by the integral equation, and finally the radar cross section is obtained by the summation of these modes. The traditional method used to solve a homogeneous dielectric BOR with integral equations is the Method of Moments (MoM) [13], with the memory requirement of  $\mathcal{O}(N^2)$ , where  $N$  is the number of unknowns. It is still time consuming for large-scale BOR problems with the MoM. The computational time consumed in solving the integral equation of the BOR problem mainly depends on the evaluation of modal Green's function (MGF). Much research have been done to solve this problem. Gedney and Mittra used the fast Fourier transform (FFT) to enhance the computational efficiency of the Method of Moments [14]. Abdelmageed and Mohsen used Bartky's transformation and spherical Bessel function expansion to evaluate the modal Green's functions [15,16]. Yu *et al.* also use spherical Bessel functions to expand the MGF and obtain near-axis far-distance closed-form MGFs [17].

In this work, we extend the fast inhomogeneous plane wave algorithm (FIPWA) [18,19] to accelerate the computation of the MoM for homogeneous dielectric bodies of revolution. PMCHW (Poggio, Miller, Chang, Harrington, Wu) integral equation [20–22] is used for solving the problem of a homogeneous dielectric scatterer excited by plane waves in the free space. The aggregation and disaggregation factors can be computed efficiently due to the cylindrical harmonics decomposition. Both the memory requirement and the CPU time are saved for large scale BOR problems. Numerical results are given to demonstrate the validity and efficiency of the FIPWA method. This method also can be used to solve perfect electric conducting (PEC) BOR problems and composite BOR problems with both dielectric and PEC objects.

## 2 Integral equation for body of revolution

### 2.1 PMCHW integral equations for a dielectric BOR object

The scattering of electromagnetic waves from a homogeneous dielectric object having permittivity  $\epsilon_2$  and permeability  $\mu_2$  in a homogeneous background medium ( $\epsilon_1, \mu_1$ ) can be solved by PMCHW (Poggio, Miller, Chang, Harrington, Wu) integral equations as follows:

$$\hat{n} \times \mathbf{E}_{inc} = \hat{n} \times [L_1(\mathbf{J}) + L_2(\mathbf{J})] - \hat{n} \times [K_1(\mathbf{M}) + K_2(\mathbf{M})], \quad (2.1)$$

$$\hat{n} \times \mathbf{H}_{inc} = \hat{n} \times \left\{ [K_1(\mathbf{J}) + K_2(\mathbf{J})] + \left[ \frac{1}{\eta_1^2} L_1(\mathbf{M}) + \frac{1}{\eta_2^2} L_2(\mathbf{M}) \right] \right\}, \quad (2.2)$$

where  $\mathbf{J}$  and  $\mathbf{M}$  are the induced electric and magnetic current densities,  $\eta_i = \sqrt{\mu_i/\epsilon_i}$  is the wave impedance for region  $i$  ( $i=1,2$ ),  $\mathbf{E}_{inc}$  and  $\mathbf{H}_{inc}$  are the incident electric field and incident magnetic field, respectively. The operators  $L_i$  and  $K_i$  are defined as

$$L_i(\mathbf{x}) = j\omega\mu_i \int_S \left[ \mathbf{x}G_i + \frac{1}{\omega^2\mu_i\epsilon_i} \nabla \nabla \cdot \mathbf{x}G_i \right] ds, \quad (2.3)$$

$$K_i(\mathbf{x}) = \int_S \mathbf{x} \times \nabla G_i ds, \quad (2.4)$$

where  $S$  is the surface of the scatterer, and  $G_i$  is the scalar Green's function of background medium ( $i=1$ ) or dielectric region ( $i=2$ ) expressed as

$$G_i(\mathbf{r}, \mathbf{r}') = \frac{e^{-jk_i|\mathbf{r}-\mathbf{r}'|}}{4\pi|\mathbf{r}-\mathbf{r}'|} \quad (2.5)$$

with  $k_i = \omega \sqrt{\mu_i \varepsilon_i}$ .

In order to solve PMCHW integral equations, the unknown surface current densities are expanded by basis functions

$$\mathbf{J}(\mathbf{r}) = \sum_{q=1}^N J_q \mathbf{f}_q(\mathbf{r}), \quad (2.6)$$

$$\mathbf{M}(\mathbf{r}) = \sum_{q=1}^N M_q \mathbf{f}_q(\mathbf{r}), \quad (2.7)$$

where  $2N$  is the number of the unknowns. Using the Galerkin's method, we can rewrite the PMCHW integral equations as

$$(P_1 + P_2)[\mathbf{J}] - (Q_1 + Q_2)[\mathbf{M}] = b^{TE}, \quad (2.8)$$

$$(Q_1 + Q_2)[\mathbf{J}] - \left( \frac{1}{\eta_1^2} P_1 + \frac{1}{\eta_2^2} P_2 \right) [\mathbf{M}] = b^{TH}, \quad (2.9)$$

$$(P_i)_{pq} = \langle \mathbf{f}_p, L_i(\mathbf{f}_q) \rangle, \quad (2.10)$$

$$(Q_i)_{pq} = \langle \mathbf{f}_p, K_i(\mathbf{f}_q) \rangle, \quad (2.11)$$

$$b_p^{TE} = \langle \mathbf{f}_p, \mathbf{E}_{inc} \rangle, \quad (2.12)$$

$$b_p^{TH} = \langle \mathbf{f}_p, \mathbf{H}_{inc} \rangle, \quad (2.13)$$

where  $\mathbf{f}_q$  is the basis function and  $\mathbf{f}_p$  is the testing function.

## 2.2 Body of revolution

The surface of the BOR is generated by revolving a plane curve about the  $z$ -axis. The surface and the curve are shown in Fig. 1. Here  $\rho, \phi, z$  are the cylindrical coordinate variables, and  $t$  is arc length along the generatrix. We define the induced current as expansions (2.6) and (2.7) to approximate an arbitrary  $\mathbf{J}$  and  $\mathbf{M}$  on  $S$ :

$$\mathbf{J} = \sum_{m,i} (J_{mi}^t \mathbf{f}_{mi}^t + J_{mi}^\phi \mathbf{f}_{mi}^\phi), \quad (2.14)$$

$$\mathbf{M} = \sum_{m,i} (M_{mi}^t \mathbf{f}_{mi}^t + M_{mi}^\phi \mathbf{f}_{mi}^\phi), \quad (2.15)$$

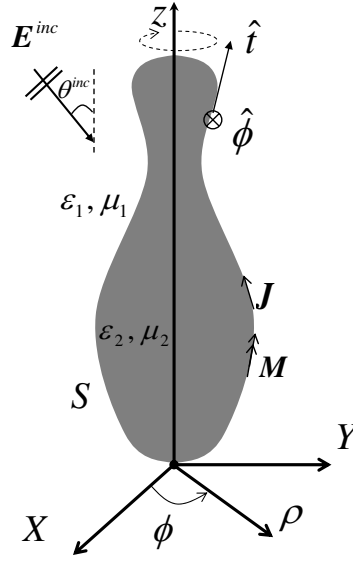


Figure 1: A body of revolution and the coordinate system, where  $\theta^{inc}$  is the angle of incident wave, and  $\hat{t}$  and  $\hat{\phi}$  are the unit vectors along the generatrix and azimuthal direction, respectively.

where  $\mathbf{f}_{mi}^\alpha = \hat{\alpha} f_i(t) e^{jm\phi}$  is the basis function,  $\alpha = t$  or  $\phi$ ,  $\hat{t} = \hat{x} \sin\theta \cos\phi + \hat{y} \sin\theta \sin\phi + \hat{z} \cos\theta$  ( $t$ -directed unit vector),  $\hat{\phi} = -\hat{x} \sin\phi + \hat{y} \cos\phi$  ( $\phi$ -directed unit vector); here  $\theta$  and  $\phi$  are the elevation and azimuthal angles in the spherical coordinate system, and  $f_i(t) = \frac{1}{\rho} T_i(t)$ , where  $T_i$  is the triangular function

$$T_i(t) = \begin{cases} \frac{t-t_{i-1}}{t_i-t_{i-1}}, & \text{if } t \in [t_{i-1}, t_i], \\ \frac{t_{i+1}-t}{t_{i+1}-t_i}, & \text{if } t \in [t_i, t_{i+1}], \\ 0, & \text{otherwise.} \end{cases} \quad (2.16)$$

Because of the rotational symmetry, the solution becomes a Fourier series in  $\phi$ , and each term is uncoupled to every other term because of the orthogonality. The expansion functions chosen for the solution are harmonic in  $\phi$  (azimuth angle) and subsectional in  $t$  (contour length variable). The testing function is

$$\mathbf{W}_{ni}^\alpha = \hat{\alpha} f_i(t) e^{-jn\phi}, \quad (2.17)$$

where the testing function  $\mathbf{W}_{ni}^\alpha$  are orthogonal to  $\mathbf{f}_{mi}^\alpha$ ,  $m \neq n$ , over 0 to  $2\pi$  on  $\phi$ , and also to  $L(\mathbf{f}_m)$  and  $K(\mathbf{f}_m)$  (the field from  $\mathbf{f}_m$ ). So all impedance elements are zero except for those  $m = n$ , and each mode can be treated separately. For each mode, we have to solve the following matrix equation:

$$\begin{bmatrix} Z_n^{EE} & Z_n^{EH} \\ Z_n^{HE} & Z_n^{HH} \end{bmatrix} \cdot \begin{bmatrix} J_n \\ M_n \end{bmatrix} = \begin{bmatrix} V_n^E \\ V_n^H \end{bmatrix}. \quad (2.18)$$

In order to balance the impedance elements [23], the matrix equation can be rewritten as

$$\begin{bmatrix} Z_n^{EE} & \eta_1 Z_n^{EH} \\ \eta_1 Z_n^{HE} & \eta_1^2 Z_n^{HH} \end{bmatrix} \cdot \begin{bmatrix} J_n \\ M_n/\eta_1 \end{bmatrix} = \begin{bmatrix} V_n^E \\ \eta_1 V_n^H \end{bmatrix}. \quad (2.19)$$

Each of the element in the above impedance matrix is actually a submatrix; for example

$$Z_n^{EE} = \begin{bmatrix} Z_n^{tt,EE} & Z_n^{t\phi,EE} \\ Z_n^{\phi t,EE} & Z_n^{\phi\phi,EE} \end{bmatrix}, \quad (2.20)$$

where superscripts  $t$  and  $\phi$  denote the  $t$  and  $\phi$  components of the basis and testing functions, respectively. Similar expressions can be written for  $Z_n^{EH}$ ,  $Z_n^{HE}$ , and  $Z_n^{HH}$ .

The detail for the above impedance elements can be found in [7], for example,

$$\begin{aligned} (Z_n^{tt})_{pq}^{EE} = & \int dt' \int dt \left[ j\omega\mu_1 T_p(t') T_q(t) \left( \cos\theta \cos\theta' g_n^1 \right. \right. \\ & \left. \left. + \sin\theta \sin\theta' \frac{g_{n+1}^1 + g_{n-1}^1}{2} \right) + \frac{1}{j\omega\varepsilon_1} T_p(t') T_q(t) g_n^1 \right] \\ & + \int dt' \int dt \left[ j\omega\mu_2 T_p(t') T_q(t) \left( \cos\theta \cos\theta' g_n^2 \right. \right. \\ & \left. \left. + \sin\theta \sin\theta' \frac{g_{n+1}^2 + g_{n-1}^2}{2} \right) + \frac{1}{j\omega\varepsilon_2} T_p(t') T_q(t) g_n^2 \right], \end{aligned} \quad (2.21)$$

where  $p$  and  $q$  are the indices of the basis and testing functions; the modal Green's function (MGF)  $g_n^i$  ( $i=1,2$ ) can be expressed as

$$g_n^i = \int_0^\pi \frac{e^{-jk_i R_0}}{R_0} \cos n\phi d\phi, \quad (2.22)$$

$$R_0 = \sqrt{\rho^2 + \rho'^2 - 2\rho\rho' \cos\phi + (z-z')^2}. \quad (2.23)$$

For the traditional MoM, the modal Green's function has to be evaluated by a numerical method, hence it is time consuming when the radius of the BOR is large. Many works have been done to improve the efficiency of the MGF.

### 2.3 Fast inhomogeneous plane wave algorithm

As mentioned above, it is time consuming to solve the MGF, and the memory requirement for MoM is  $\mathcal{O}(N^2)$ , where  $N$  is the number of the unknowns. The fast inhomogeneous plane wave algorithm (FIPWA) was first proposed for 2-D and 3-D integral equations in [18,19], and then applied to accelerate the computation of the MoM for PEC bodies of revolution in [24], which is a special 3-D problem with axial symmetry. Here we

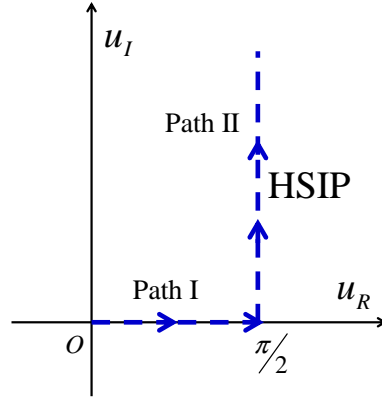


Figure 2: The half Sommerfeld integration path on the complex  $u$  plane. Path I is  $(u_R = 0 \sim \frac{\pi}{2}, u_I = 0)$ , and Path II is  $(u_R = \frac{\pi}{2}, u_I = 0 \sim \infty)$ .

extend this method to dielectric BOR. Based on Weyl identity [25], the Green's function can be expressed as

$$\begin{aligned} \frac{e^{-jkr_{pq}}}{r_{pq}} &= \frac{1}{j} \int_0^{\infty} dk_{\rho} \frac{k_{\rho}}{k_z} J_0(k_{\rho} \rho_{pq}) e^{-jk_z |z_{pq}|} \\ &= \frac{k}{j2\pi} \int_0^{2\pi} dv \int_{HSIP} du \sin u e^{-jk\hat{k} \cdot \mathbf{r}_{pq}}, \end{aligned} \quad (2.24)$$

where  $\hat{k} = \hat{x} \sin u \cos v + \hat{y} \sin u \sin v + \hat{z} \cos u$ ,  $k_{\rho} = k \sin u$ ,  $k_z = k \cos u$ , and  $\mathbf{r}_{pq} = \mathbf{r}_p - \mathbf{r}_q$ . Here  $\mathbf{r}_q$  is the source point and  $\mathbf{r}_p$  is the field point. In the following part, they are also named sub-scatterers. The integration of the variable  $u$  in Eq. (2.24) is computed along the half Sommerfeld integration path (HSIP) in Fig. 2. It is important to note that the variable  $u = u_R + ju_I$  is complex here.  $e^{-jk\hat{k} \cdot \mathbf{r}_{pq}}$  is called the inhomogeneous plane wave by Jackson [26]. When the variable  $u$  and  $v$  are real, it is called a homogeneous plane wave. So Eq. (2.24) can be viewed as the summation of inhomogeneous plane waves in different directions, which are expressed by  $\hat{k}(u, v)$ , and weighted by  $\sin u$ . In order to realize the Fast Inhomogeneous Plane Wave Algorithm (FIPWA), the basis functions are divided into groups. Here we call  $\mathbf{r}_m$  and  $\mathbf{r}'_m$  the centers of the groups which contain the source point  $\mathbf{r}_q$  and field point  $\mathbf{r}_p$  respectively. As shown in Fig. 3,  $\mathbf{r}_{pq} = \mathbf{r}_{pm} + \mathbf{r}_{mm'} + \mathbf{r}_{m'q}$ . Eq. (2.24) can be rewritten as

$$\begin{aligned} \frac{e^{-jkr_{pq}}}{r_{pq}} &= \frac{k}{j2\pi} \int_0^{2\pi} dv \int_{HSIP} du \sin u e^{-jk\hat{k} \cdot (\mathbf{r}_{pm} + \mathbf{r}_{mm'} + \mathbf{r}_{m'q})} \\ &= \frac{k}{j2\pi} \int_0^{2\pi} dv \int_{HSIP} du \sin u e^{-j\mathbf{k} \cdot \mathbf{r}_{pm}} \cdot e^{-j\mathbf{k} \cdot \mathbf{r}_{mm'}} \cdot e^{-j\mathbf{k} \cdot \mathbf{r}_{m'q}}. \end{aligned} \quad (2.25)$$

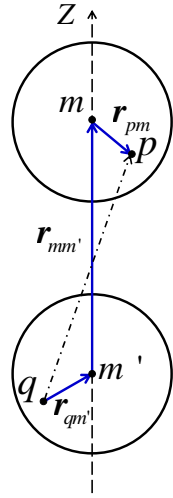


Figure 3: The grouping of the source point  $\mathbf{r}_q$  and the field point  $\mathbf{r}_p$ , where  $\mathbf{r}'_m$  is the center of source group, and  $\mathbf{r}_m$  is the center of the field group. The group centers  $\mathbf{r}'_m$  and  $\mathbf{r}_m$  are in the  $z$  direction.

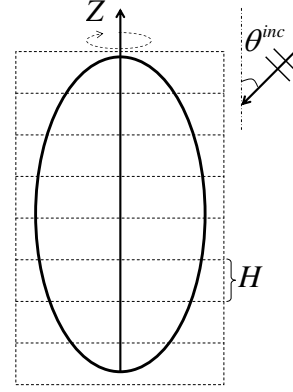


Figure 4: The division of groups in the  $z$  direction, where  $H$  is the height of each group.

The basis functions are divided into  $M$  groups along the  $z$  direction as shown in Fig. 4. In this way,  $\mathbf{r}_{mm'}$  has  $\hat{z}$  component only,  $\mathbf{r}_{mm'} = \hat{z}z_{mm'}$ . This property will make the integrand decay exponentially away from the real axis in the  $u$  plane. In order to perform the integration along the HSIP, Eq. (2.25) can be rewritten as

$$\frac{e^{-jk r_{pq}}}{r_{pq}} = \int_0^{2\pi} dv \int_{HSIP} du f(u) B_{pm}(u, v) e^{-jk z_{mm'} \cos u} B_{m'q}(u, v), \quad (2.26)$$

where

$$\begin{aligned} f(u) &= \frac{k}{j2\pi} \sin u, \\ B_{pm}(u, v) &= e^{-jk \hat{k} \cdot \mathbf{r}_{pm}}, \\ B_{m'q}(u, v) &= e^{-jk \hat{k} \cdot \mathbf{r}_{m'q}}. \end{aligned}$$

Here  $B_{pm}(u, v)$  and  $B_{m'q}(u, v)$  represent the radiation and receiving patterns for the field and source groups, respectively. And  $f(u)$  can be considered as the weight function. Both  $B_{pm}(u, v)$  and  $B_{m'q}(u, v)$  are inhomogeneous plane waves as  $u$  is complex. With proper numerical quadrature methods for  $u$  and  $v$ , the integral can be expressed as

$$\begin{aligned} \frac{e^{-jk r_{pq}}}{r_{pq}} &= \sum_{s_2} \sum_{s_1} B_{pm}(u_{s_1}, v_{s_2}) B_{m'q}(u_{s_1}, v_{s_2}) T_{mm'}(u_{s_1}, v_{s_2}) \\ &= \sum_{\Omega_s} B_{pm}(\Omega_s) B_{m'q}(\Omega_s) T_{mm'}(\Omega_s), \end{aligned} \quad (2.27)$$

where

$$\begin{aligned}\Omega_s &= (u_{s_1}, v_{s_2}), \\ T_{mm'}(u_{s_1}, v_{s_2}) &= w_1 w_2 \frac{-jk}{2\pi} \sin u_{s_1} e^{-jkz_{mm'} \cos u_{s_1}},\end{aligned}$$

$u_{s_1}$  and  $v_{s_2}$  are the integration points for  $u$  and  $v$ ,  $w_1$  and  $w_2$  are the weights for  $u$  and  $v$ , respectively. Eq. (2.27) can be interpreted as the summation of inhomogeneous plane waves translated from the source group to the field group. Substituting Eq. (2.27) into Eqs. (2.8)-(2.9), we obtain

$$P_{pq}^i = \frac{k_i^2 \eta_i}{8\pi^2} \int_0^{2\pi} \int_{\text{HSIP}} \mathbf{V}_{fmp}^{iP} T_{mm'}^i \mathbf{V}_{sm'q}^{iP} dudv, \quad (2.28)$$

$$Q_{pq}^i = -\frac{k_i^2}{8\pi^2} \int_0^{2\pi} \int_{\text{HSIP}} \mathbf{V}_{fmp}^{iQ} T_{mm'}^i \mathbf{V}_{sm'q}^{iQ} dudv, \quad (2.29)$$

where the half Sommerfeld integration path (HSIP) is shown in Fig. 2, and the aggregation factor  $\mathbf{V}_{sm'q}^{iP}$ ,  $\mathbf{V}_{sm'q}^{iQ}$  and disaggregation factor  $\mathbf{V}_{fmp}^{iP}$ ,  $\mathbf{V}_{fmp}^{iQ}$  can be expressed as

$$\mathbf{V}_{sm'q}^{iP}(u_{s_1}, v_{s_2}) = \int_S ds B_{m'q}^i(u_{s_1}, v_{s_2}) \mathbf{f}_q(\mathbf{r}_{m'q}), \quad (2.30)$$

$$\mathbf{V}_{sm'q}^{iQ}(u_{s_1}, v_{s_2}) = \int_S ds B_{m'q}^i(u_{s_1}, v_{s_2}) \mathbf{f}_q(\mathbf{r}_{m'q}), \quad (2.31)$$

$$\mathbf{V}_{fmp}^{iP}(u_{s_1}, v_{s_2}) = \int_S ds B_{pm}^i(u_{s_1}, v_{s_2}) [\bar{\mathbf{I}} - \hat{\mathbf{k}}\hat{\mathbf{k}}] \cdot \mathbf{W}_p(\mathbf{r}_{pm}), \quad (2.32)$$

$$\mathbf{V}_{fmp}^{iQ}(u_{s_1}, v_{s_2}) = \int_S ds B_{pm}^i(u_{s_1}, v_{s_2}) \hat{\mathbf{k}} \times \mathbf{W}_p(\mathbf{r}_{pm}). \quad (2.33)$$

From Eqs. (2.30)-(2.33), it is clear that

$$\mathbf{V}_{sm'q}^{iP} = \mathbf{V}_{sm'q}^{iQ}, \quad \mathbf{V}_{fmp}^{iQ} = \hat{\mathbf{k}} \times \mathbf{V}_{fmp}^{iP}.$$

As  $\int_S ds = \int_t dt \int_0^{2\pi} d\phi \rho(t)$ , the traditional MoM performs the integration of  $\phi$  numerically, thus this part takes most of the computational time in MoM. After substituting the basis and testing functions into Eqs. (2.30) and (2.32), the aggregation and disaggregation factors can be derived as

$$\mathbf{V}_{sm'q}^{iP}(u_{s_1}, v_{s_2}) = \int dt \int_0^{2\pi} d\phi \rho_q(t) B_{m'q}^i(u_{s_1}, v_{s_2}) \hat{\mathbf{a}}_\alpha f_q(t) e^{jn\phi}, \quad (2.34)$$

$$\mathbf{V}_{fmp}^{iP}(u_{s_1}, v_{s_2}) = \int dt \int_0^{2\pi} d\phi \rho_p(t) B_{pm}^i(u_{s_1}, v_{s_2}) [\bar{\mathbf{I}} - \hat{\mathbf{k}}\hat{\mathbf{k}}] \cdot \hat{\mathbf{a}}_\alpha f_p(t) e^{-jn\phi}. \quad (2.35)$$

From the integral representation of Bessel function

$$J_n(z) = \frac{j^{-n}}{2\pi} \int_0^{2\pi} e^{jz\cos\phi} e^{jn\phi} d\phi, \tag{2.36}$$

$$J_n(z) = \frac{j^{-n}}{\pi} \int_0^\pi e^{jz\sin\phi} \cos(n\phi) d\phi, \tag{2.37}$$

$$J_n(z) = \frac{1}{\pi} \int_0^\pi \cos(z\sin\phi - n\phi) d\phi, \tag{2.38}$$

the above  $\phi$  integration can be carried out analytically, and then the aggregation and disaggregation factors can be simplified as

$$\begin{aligned} \mathbf{V}_{fmp}^{iPt} = \int dt e^{-j\mathbf{k}_i \mathbf{r}_m} e^{-jk_i \cos u z_p} e^{-jnv} \cdot \left\{ \cos u \sin \theta \left[ \frac{\pi}{j^{n+1}} J_{n+1}(\zeta_p) + \frac{\pi}{j^{n-1}} J_{n-1}(\zeta_p) \right] \hat{u} \right. \\ \left. - \sin u \cos \theta \frac{2\pi}{j^n} J_n(\zeta_p) \hat{u} + \sin \theta \left[ \frac{\pi}{j^n} J_{n-1}(\zeta_p) - \frac{\pi}{j^{n+2}} J_{n+1}(\zeta_p) \right] \hat{v} \right\}, \end{aligned} \tag{2.39}$$

$$\begin{aligned} \mathbf{V}_{fmp}^{iP\phi} = \int dt e^{-j\mathbf{k}_i \mathbf{r}_m} e^{-jk_i \cos u z_p} e^{-jnv} \cdot \left\{ -\cos u \left[ \frac{\pi}{j^n} J_{n-1}(\zeta_p) - \frac{\pi}{j^{n+2}} J_{n+1}(\zeta_p) \right] \hat{u} \right. \\ \left. + \left[ \frac{\pi}{j^{n+1}} J_{n+1}(\zeta_p) + \frac{\pi}{j^{n-1}} J_{n-1}(\zeta_p) \right] \hat{v} \right\}, \end{aligned} \tag{2.40}$$

$$\begin{aligned} \mathbf{V}_{sm'q}^{iPt} = \int dt e^{-j\mathbf{k}_i \mathbf{r}_{m'}} e^{jk_i \cos u z_q} e^{jnv} \cdot \left\{ \cos u \sin \theta \left[ \frac{\pi}{j^{-(n+1)}} J_{n+1}(\zeta_q) + \frac{\pi}{j^{-(n-1)}} J_{n-1}(\zeta_q) \right] \hat{u} \right. \\ \left. - \sin u \cos \theta \frac{2\pi}{j^{-n}} J_n(\zeta_q) \hat{u} + \sin \theta \left[ \frac{\pi}{j^{-n}} J_{n+1}(\zeta_q) + \frac{\pi}{j^{-(n-2)}} J_{n-1}(\zeta_q) \right] \hat{v} \right\}, \end{aligned} \tag{2.41}$$

$$\begin{aligned} \mathbf{V}_{sm'q}^{iP\phi} = \int dt e^{-j\mathbf{k}_i \mathbf{r}_{m'}} e^{jk_i \cos u z_q} e^{jnv} \cdot \left\{ \cos u \left[ \frac{\pi}{j^{-n}} J_{n+1}(\zeta_q) - \frac{\pi}{j^{-(n-2)}} J_{n-1}(\zeta_q) \right] \hat{u} \right. \\ \left. - \left[ \frac{\pi}{j^{-n-1}} J_{n+1}(\zeta_q) + \frac{\pi}{j^{-(n-1)}} J_{n-1}(\zeta_q) \right] \hat{v} \right\}, \end{aligned} \tag{2.42}$$

where  $\zeta_i = k\rho_i \sin u$ . This will greatly reduce the CPU time. In the aggregation factor,

$$e^{-jk_i \rho_{m'} \sin u \cos(v - \phi_{m'})} e^{jnv}$$

can be extracted, while in disaggregation factor

$$e^{jk_i \rho_m \sin u \cos(v - \phi_{m'})} e^{-jnv}$$

can be extracted. As the group centers are all on the z axis,

$$\rho_m = \rho_{m'} = 0,$$

these extracted items can be canceled out. After this is done, it is clear that there is no variable  $v$  either in aggregation or disaggregation factors. So these factors are  $v$  independent, and can be rewritten as

$$\mathbf{V}_{fmp}^{iPt} = \int dt e^{-j\mathbf{k}_i \mathbf{r}_m} e^{-jk_i \cos u z_p} \cdot \left\{ \cos u \sin \theta \left[ \frac{\pi}{j^{n+1}} J_{n+1}(\zeta_p) + \frac{\pi}{j^{n-1}} J_{n-1}(\zeta_p) \right] \hat{u} - \sin u \cos \theta \frac{2\pi}{j^n} J_n(\zeta_p) \hat{u} + \sin \theta \left[ \frac{\pi}{j^n} J_{n-1}(\zeta_p) - \frac{\pi}{j^{n+2}} J_{n+1}(\zeta_p) \right] \hat{v} \right\}, \quad (2.43)$$

$$\mathbf{V}_{fmp}^{iP\phi} = \int dt e^{-j\mathbf{k}_i \mathbf{r}_m} e^{-jk_i \cos u z_p} \cdot \left\{ -\cos u \left[ \frac{\pi}{j^n} J_{n-1}(\zeta_p) - \frac{\pi}{j^{n+2}} J_{n+1}(\zeta_p) \right] \hat{u} + \left[ \frac{\pi}{j^{n+1}} J_{n+1}(\zeta_p) + \frac{\pi}{j^{n-1}} J_{n-1}(\zeta_p) \right] \hat{v} \right\}, \quad (2.44)$$

$$\mathbf{V}_{sm'q}^{iPt} = \int dt e^{-j\mathbf{k}_i \mathbf{r}_{m'}} e^{jk_i \cos u z_q} \cdot \left\{ \cos u \sin \theta \left[ \frac{\pi}{j^{-(n+1)}} J_{n+1}(\zeta_q) + \frac{\pi}{j^{-(n-1)}} J_{n-1}(\zeta_q) \right] \hat{u} - \sin u \cos \theta \frac{2\pi}{j^{-n}} J_n(\zeta_q) \hat{u} + \sin \theta \left[ \frac{\pi}{j^{-n}} J_{n+1}(\zeta_q) + \frac{\pi}{j^{-(n-2)}} J_{n-1}(\zeta_q) \right] \hat{v} \right\}, \quad (2.45)$$

$$\mathbf{V}_{sm'q}^{iP\phi} = \int dt e^{-j\mathbf{k}_i \mathbf{r}_{m'}} e^{jk_i \cos u z_q} \cdot \left\{ \cos u \left[ \frac{\pi}{j^{-n}} J_{n+1}(\zeta_q) - \frac{\pi}{j^{-(n-2)}} J_{n-1}(\zeta_q) \right] \hat{u} - \left[ \frac{\pi}{j^{-(n-1)}} J_{n+1}(\zeta_q) + \frac{\pi}{j^{-(n-1)}} J_{n-1}(\zeta_q) \right] \hat{v} \right\}. \quad (2.46)$$

Moreover,  $\Omega_s = \{u_{s1}\}$  because no  $v$  integration is needed.

Gauss-Legendre quadrature is used in Path I, and Gauss-Laguerre quadrature is used in Path II for the integration along the HSIP in (2.26). It is worth noting that the number of the quadrature samples needed is proportional to the group size for the radiation pattern of each group. Assume that  $\Omega_s = \{u_{s1}\}$  is the quadrature samples for the radiation pattern,  $\Omega_t = \{u_{t1}\}$  is the quadrature samples for the translation factor. When the distance between the group centers is larger than the group size, the number of  $\Omega_t$  (which is decided by the distance between the group centers) is larger than the number of  $\Omega_s$ , hence Eq. (2.27) needs to use  $\Omega_t$  to guarantee accuracy, hence it will cost more memory. To solve this kind of problem, Eq. (2.27) can be rewritten as

$$\begin{aligned} \frac{e^{-jkr_{pq}}}{r_{pq}} &= \sum_{\Omega_t} B_{pm}(\Omega_t) B_{m'q}(\Omega_t) T_{mm'}(\Omega_t) \\ &= \sum_{\Omega_t} T_{mm'}(\Omega_t) \sum_{\Omega_s} I(\Omega_t, \Omega_s) B_{pm}(\Omega_s) B_{m'q}(\Omega_s) \\ &= \sum_{\Omega_s} B_{pm}(\Omega_s) B_{m'q}(\Omega_s) \sum_{\Omega_t} T_{mm'}(\Omega_t) I(\Omega_t, \Omega_s) \\ &= \sum_{\Omega_s} B_{pm}(\Omega_s) B_{m'q}(\Omega_s) T'_{mm'}(\Omega_s), \end{aligned} \quad (2.47)$$

where

$$I(\Omega_t, \Omega_s) = \prod_{j=0, j \neq k}^n \left( \frac{\Omega_t - \Omega_{sj}}{\Omega_{sk} - \Omega_{sj}} \right)$$

and

$$T'_{mm'}(\Omega_s) = \sum_{\Omega_t} T_{mm'}(\Omega_t) I(\Omega_t, \Omega_s).$$

This interpolation can be done efficiently because  $T_{mm'} = T_{m-m'}$ . The number of the sample points along Path I and Path II is decided by  $M_u = kD + (kD)^{1/3}$  [19], and numerical tests shows that  $H = 0.3\lambda$  is a good dividing height for each group, see Fig. 4.

### 3 Numerical results

In this section, some numerical results are presented to show the validity of the proposed FIPWA. All problems are solved on the same computer (Intel Core2 Duo CPU P8400 @ 2.26GHz with 1.92GB RAM) in order to make a fair comparison, with only one core being used.

First of all, a homogeneous dielectric sphere ( $\epsilon_r = 4.0$ ,  $\mu_r = 1.0$ ) with a radius 50 m is simulated at 150MHz by the BOR-FIPWA and BOR-MoM and the results are compared with MIE series solution. As shown in Fig. 5, bistatic RCS results agree well among these three sets of results.

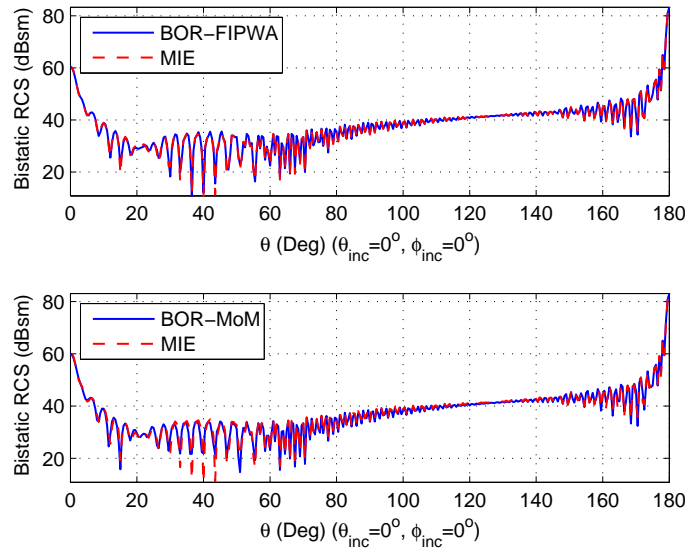


Figure 5: Bistatic radar cross section of a homogeneous dielectric sphere ( $\epsilon_r = 4.0$ ,  $\mu_r = 1.0$ ) with the radius 50 m. The incident wave at 150MHz has horizontal polarization ( $\theta^{inc} = 0^\circ$ ,  $\phi^{inc} = 0^\circ$ ,  $\theta^{sca} = 0^\circ \sim 180^\circ$ ,  $\phi^{sca} = 0^\circ$ ).

Table 1: The memory requirement and CPU time comparison of homogeneous dielectric spheres ( $\epsilon_r = 4.0, \mu_r = 1.0$ ) with different number of unknowns (thus the electrical size). The incident wave is  $\lambda_0 = 2$  m with horizontal polarization.

Radius (m)	Unknowns	MoM		FIPWA	
		Memory (MB)	CPU Time (s)	Memory (MB)	CPU Time (s)
5	784	4.68	138	1.48	35
8	1256	12.04	560	3.59	105
10	1568	18.76	980	5.45	167
20	3140	75.24	8783	21.4	630
50	7852	470.4	-	128.5	3597

In order to test the efficiency of the proposed method, homogeneous dielectric spheres ( $\epsilon_r = 4.0, \mu_r = 1.0$ ) with different electric sizes are computed by the BOR-FIPWA and BOR-MoM. All of the spheres are excited by the plane wave with horizontal polarization ( $\theta^{inc} = 0^\circ, \phi^{inc} = 0^\circ, \lambda_0 = 1$  m). The CPU time to fill the impedance matrix and the memory requirement are listed in Table 1. As shown in Fig. 6, the memory requirement is  $\mathcal{O}(N^2)$  for the BOR-MoM, where  $N$  is the number of unknowns. For the BOR-FIPWA, as the number of sample points along the HSIP is nearly proportional to the radius of the BOR, the complexity of the memory requirement is slightly less than  $\mathcal{O}(N^2)$ . As shown in Fig. 7, the CPU time for system creation of the BOR-FIPWA is compared with BOR-MoM. It is clear that the CPU time for computing the modal Green's function (MGF) in MoM is proportional to the number of integration points in the  $\phi$  direction, which is decided by the radius of the BOR. So it is reasonable that the CPU time complexity for BOR-MoM (dielectric sphere) is  $\mathcal{O}(N^3)$ . For BOR-FIPWA, it is about  $\mathcal{O}(N^2)$ , as mentioned above.

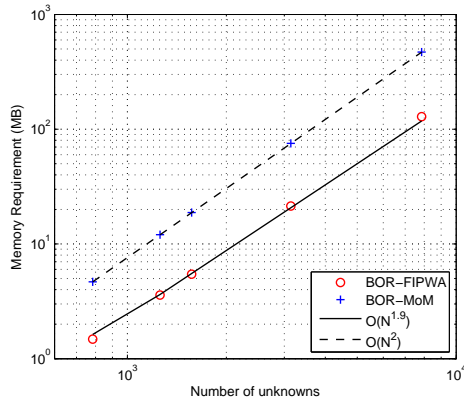


Figure 6: The memory requirement comparison of homogeneous dielectric spheres ( $\epsilon_r = 4.0, \mu_r = 1.0$ ) with different number of unknowns (thus the electrical size).

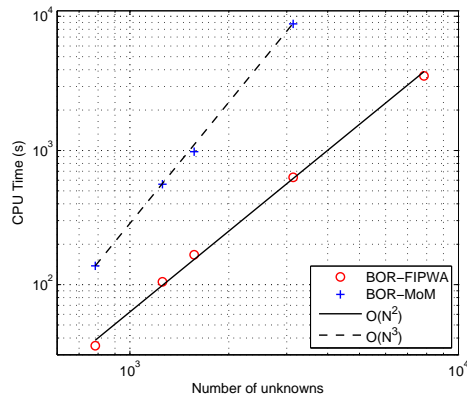
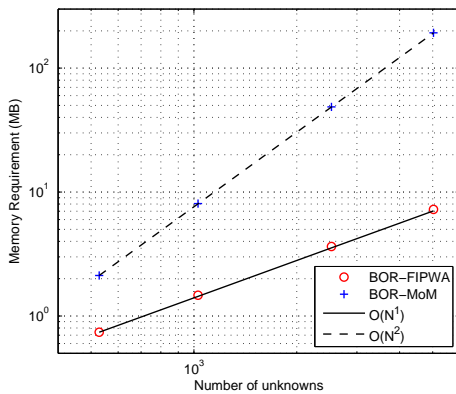
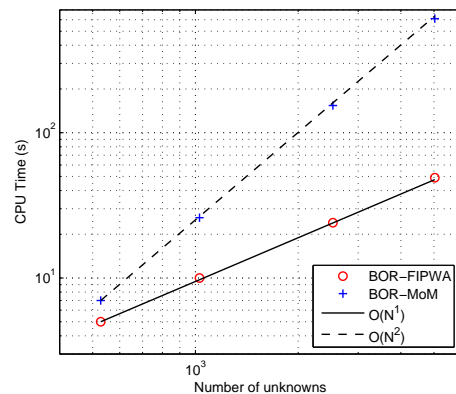


Figure 7: The CPU time comparison of homogeneous dielectric spheres ( $\epsilon_r = 4.0, \mu_r = 1.0$ ) with different number of unknowns (thus the electrical size).

Table 2: The memory requirement and CPU time comparison of PEC cylinder with the same radius ( $r=0.25$  m) and different height.

height (m)	Unknowns	MoM		FIPWA	
		Memory (MB)	CPU Time (s)	Memory (MB)	CPU Time (s)
10	528	2.12	7	0.74	5
20	1028	8.08	26	1.47	10
50	2528	48.7	154	3.64	24
100	5028	192.8	610	7.25	49

For homogeneous dielectric sphere problems, the number of unknowns and the number of sample points along the HSIP are both proportional to the electrical size. On the other hand, if the radius of the object is fixed, the BOR-FIPWA will perform even better. For example, homogeneous dielectric cylinders ( $\epsilon_r = 4.0$ ,  $\mu_r = 1.0$ ) with a fixed radius ( $r = 0.25$  m) and different heights are computed by the BOR-FIPWA and BOR-MoM. All of the homogeneous dielectric cylinders are excited by the plane wave with horizontal polarization ( $\theta^{inc} = 90^\circ$ ,  $\phi^{inc} = 0^\circ$ ,  $\lambda_0 = 2$  m). The CPU time for system creation and the memory requirement for each mode are listed in Table 2. As shown in Fig. 8, the memory requirement is  $\mathcal{O}(N^2)$  for the BOR-MoM. For the BOR-FIPWA, the number of sample points along the HSIP is fixed, so the complexity of the memory requirement is about  $\mathcal{O}(N)$ . As shown in Fig. 9, the CPU time for system creation of the BOR-FIPWA is compared with BOR-MoM. It is clear that the CPU time for computing the modal Green's function (MGF) is fixed. So the CPU time complexity is  $\mathcal{O}(N^2)$  for BOR-MoM (homogeneous dielectric cylinder with a fixed radius), while it is  $\mathcal{O}(N)$  for the BOR-FIPWA.

Figure 8: The memory requirement comparison of homogeneous dielectric cylinder ( $\epsilon_r = 4.0$ ,  $\mu_r = 1.0$ ) with the same radius ( $r = 0.25$  m) and different height.Figure 9: The CPU time comparison of homogeneous dielectric cylinder ( $\epsilon_r = 4.0$ ,  $\mu_r = 1.0$ ) with the same radius ( $r = 0.25$  m) and different height.

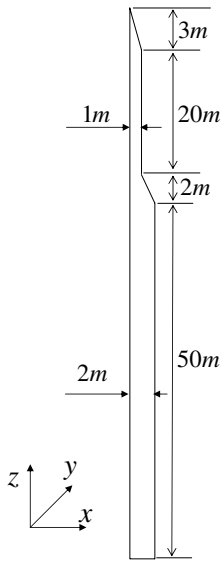


Figure 10: The geometry of a homogeneous dielectric rocket model.

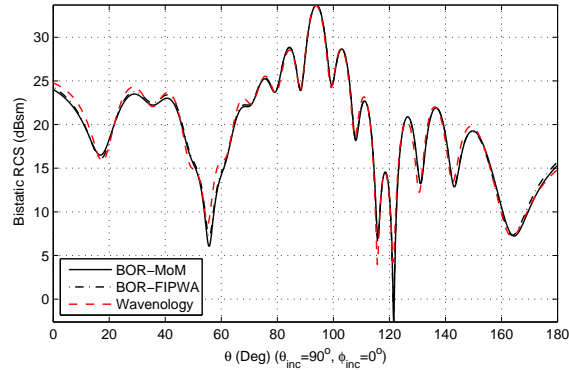


Figure 11: Bistatic radar cross section of a homogeneous rocket model ( $\epsilon_r = 9.0, \mu_r = 1.0$ ) computed by BOR-MoM, BOR-FIPWA and Wavenology. The incident wave is  $\lambda_0 = 9$  m with horizontal polarization ( $\theta^{inc} = 90^\circ, \phi^{inc} = 0^\circ, \theta^{sca} = 0^\circ \sim 180^\circ, \phi^{sca} = 0^\circ$ ).

As shown in Fig. 10, a homogeneous dielectric rocket model ( $\epsilon_r = 9.0, \mu_r = 1.0$ ) is simulated. The object is excited by the plane wave with horizontal polarization ( $\theta^{inc} = 90^\circ, \phi^{inc} = 0^\circ, \lambda_0 = 9$  m). The CPU time for system creation and the memory requirement for each mode are listed in Table 3. The bistatic RCS is shown in Fig. 11, where the BOR-FIPWA result agrees well with that from Wavenology EM [27], a software tool based on the conformal finite-difference time-domain method (rather than MoM).

Table 3: The memory requirement and CPU time comparison of the homogeneous dielectric rocket model.

Unknowns	MoM		FIPWA	
	Memory (MB)	CPU Time (s)	Memory (MB)	CPU Time (s)
1554	18.4	249	5.4	41

## 4 Conclusion

In this paper, a fast inhomogeneous plane wave algorithm is applied to solve the homogeneous dielectric BOR scattering problem. Analytical expressions for the aggregation and disaggregation factors are derived to save significant CPU time over the MoM. Although only homogeneous dielectric objects are simulated in the numerical results, this method can also be used to solve PEC BOR and combined dielectric and conducting BOR problems.

## Acknowledgments

XR and JH are supported in part by the National Science Foundation of China (No. 60971032), in part by the Programme of Introducing Talents of Discipline to Universities under Grant b07046, and in part by the Joint Ph.D. Fellowship Program of the China Scholarship Council.

## References

- [1] M. G. Andreasen, Scattering from bodies of revolution, *IEEE Trans. Antennas Propag.*, 13 (1965), 303-310.
- [2] J. R. Mautz and R. F. Harrington, Radiation and scattering from bodies of revolution, *Appl. Sci. Res.*, 20 (1969), 405-435.
- [3] T. K. Wu and L. L. Tsai, Scattering from arbitrarily-shaped lossy dielectric bodies of revolution, *Radio Sci.*, 12 (1977), 709-718.
- [4] A. W. Glisson and D. R. Wilton, Simple and efficient numerical methods for problems of electromagnetic radiation and scattering from surfaces, *IEEE Trans. Antennas Propag.*, 28 (1980), 593-603.
- [5] J. F. Hunka and K. K. Mei, Electromagnetic scattering by two bodies of revolution, *Electromagnetics*, 1 (1981), 329-347.
- [6] J. R. Mautz and R. F. Harrington, Electromagnetic coupling to a conducting body of revolution with a homogeneous material region, *Electromagnetics*, 2 (1982), 257-308.
- [7] L. N. Medgyesi-Mitschg and J. M. Putnam, Electromagnetic scattering from axially inhomogeneous bodies of revolution, *IEEE Trans. Antennas Propag.*, 32 (1984), 797-806.
- [8] P. L. Huddleston, L. N. Medgyesi-Mitschg and J. M. Putnam, Combined field integral equation formulation for scattering by dielectrically coated conducting bodies, *IEEE Trans. Antennas Propag.*, 34 (1986), 510-520.
- [9] A. A. Kishk, Y. M. M. Antar, L. Shafai, L. E. Allan, Integral equation solution of scattering from partially coated conduction bodies of revolution, *Electromagnetics*, 7 (1987), 51-60.
- [10] A. A. Kishk, G. E. Bridges, A. Sebak, L. Shafai, Integral equation solution of scattering from partially coated conduction bodies of revolution, *IEEE Trans. Magnet.*, 27 (1991), 4283-4286.
- [11] E. Y. Sun and W. V. T. Rusch, EFIE time-marching scattering from bodies of revolution and its applications, *IEEE Trans. Antennas Propag.*, 42 (1994), 412-417.
- [12] S. M. Rao, D. R. Wilton and A. W. Glisson, Electromagnetic scattering by surfaces of arbitrary shape, *IEEE Trans. Antennas Propag.*, 30 (1982), 409-418.
- [13] R. F. Harrington, *Computation by Moment Methods*, Macmillan, New York 1968.
- [14] S. D. Gedney and R. Mittra, The use of the FFT for the efficient solution of the problem of electromagnetic scattering by a body of revolution, *IEEE Trans. Antennas Propag.*, 38 (1990), 313-322.
- [15] A. K. Abdelmageed, Efficient evaluation of modal Greens functions arising in EM scattering by bodies of revolution, *Prog. Electromagn. Res.*, 27 (2000), 337-356.
- [16] A. A. K. Mohsen and A. K. Abdelmageed, A fast algorithm for treating EM scattering by bodies of revolution, *Int. J. Elect. Commun.*, 3 (2001), 164-170.
- [17] W. M. Yu, D. G. Fang and T. J. Cui, Closed form modal Green's functions for accelerated computation of bodies of revolution, *IEEE Trans. Antennas Propag.*, 56 (2008), 3452-3461.

- [18] B. Hu, W. C. Chew, E. Michielssen and J. Zhao, Fast inhomogeneous plane wave algorithm for the fast analysis of two-dimensional scattering problem, *Radio Sci.*, 34 (1999), 759-772.
- [19] B. Hu, W. C. Chew and S. Velamparambil, Fast inhomogeneous plane wave algorithm for the analysis of electromagnetic scattering, *Radio Sci.*, 36 (2001), 1327-1340.
- [20] A. J. Poggio and E. K. Miller, Integral equation solutions of three-dimensional scattering problems, *Computer Techniques for Electromagnetics*, Oxford and New York, Pergamon Press, (1973), 159-264.
- [21] R. F. Harrington, Boundary integral formulations for homogeneous material bodies, *J. Electromagn. Waves Applicat.*, 3 (1989), 1-15.
- [22] T. K. Wu and L. L. Tsai, Scattering from arbitrarily-shaped lossy dielectric bodies of revolution, *Radio Sci.*, 12 (1997), 709-718.
- [23] S. Y. Chen, J. S. Zhao and W. C. Chew, Analyzing low-frequency electromagnetic scattering from a composite object, *IEEE Trans. Geosci. Remote Sensing*, 40 (2002), 426-433.
- [24] X. Rui, J. Hu, Q. H. Liu, Fast Inhomogeneous Plane Wave Algorithm for Scattering from PEC Body of Revolution, *Microwave Opt. Technol. Lett.*, in press.
- [25] W. C. Chew, *Waves and Fields in Inhomogeneous Media*, New York 1990.
- [26] J. D. Jackson, *Classical Electrodynamics*, 2nd Edition. New York 1975.
- [27] *Wavenology EM User's Manual*, Wave Computation Technologies, Inc., 2009.